

PHASE FORMATION AND ELECTRICAL  
PROPERTIES OF SODIUM BISMUTH  
TITANATE DOPED BY BARIUM TITANATE

KHAIRUNNISA BINTI IBRAHIM

BACHELOR OF APPLIED SCIENCE (HONS)  
MATERIAL TECHNOLOGY  
UNIVERSITI MALAYSIA PAHANG

# UNIVERSITI MALAYSIA PAHANG

## DECLARATION OF THESIS AND COPYRIGHT

Author's full name : Khairunnisa binti Ibrahim

Date of birth : 22 September 1994

Title : Phase Formation and Electrical Properties of Sodium Bismuth Titanate Doped by Barium Titanate

Academic Session : Semester 1 2016/2017

I declare that this thesis is classified as:

**CONFIDENTIAL** (Contains confidential information under the Official Secret Act 1972)

**RESTRICTED** (Contains restricted information as specified by the organization where research was done)

**OPEN ACCESS** I agree that my thesis to be published as online open access (Full text)

I acknowledge that Universiti Malaysia Pahang reserve the right as follows:

1. The Thesis is the Property of Universiti Malaysia Pahang
2. The Library of Universiti Malaysia Pahang has the right to make copies for the purpose of research only.
3. The Library has the right to make copies of the thesis for academic exchange.

Certified By:

\_\_\_\_\_  
(Student's Signature)

Khairunnisa binti Ibrahim  
940922-01-5998  
Date:

\_\_\_\_\_  
(Supervisor's Signature)

Siti Aisah Binti Harun  
Date:

PHASE FORMATION AND ELECTRICAL PROPERTIES  
OF SODIUM BISMUTH TITANATE DOPED BY BARIUM  
TITANATE

KHAIRUNNISA BINTI IBRAHIM

Thesis submitted in fulfillment of the requirements  
for the award of the degree of  
Bachelor of Applied Science (Hons) Material Technology

Faculty of Industrial Sciences & Technology  
UNIVERSITI MALAYSIA PAHANG

January 2017

## **SUPERVISORS' DECLARATION**

I hereby declare that I have checked the thesis and in my opinion, this thesis is adequate in terms of scope and quality for the award of the degree of Bachelor of Applied Science (Honor) Material Technology.

Signature

Name of Supervisor : SITI AISAH BINTI HARUN

Position : SUPERVISOR

Date :

## **STUDENT'S DECLARATION**

I hereby declare that the work in this thesis is my own except for quotations and summaries which have been duly acknowledged. The thesis has not been accepted for any degree and is not concurrently submitted for award of other degree.

Signature :  
Name : **KHAIRUNNISA BINTI IBRAHIM**  
ID Number : **SC13013**  
Date :

## **DEDICATION**

This work is dedicated to my parents and sibling, Ibrahim bin Ahmad, Maznah binti Mohamed and Khairunnaseha binti Ibrahim, who have always loved me unconditionally, showed good examples that taught me to work hard for the things I dream to achieve, and fully financially supported.

This thesis work is also dedicated to my dearest friends, Nurazlin and Syakila who have been a constant source of support and encouragement during the challenges completing this work.

## ACKNOWLEDGEMENTS

I wish to thank the many people who offered their time, support and friendship to me during my studies at Universiti Malaysia Pahang. There are a number of people without whom this thesis might not have been written, and to whom I am greatly indebted.

I offer my gratitude and appreciation to my supervisors, Mdm Aisah binti Harun, for the deft ways in which you lovingly challenged and supported me through out the whole of this work - knowing when to push and when to let up.

I would always appreciate the valuable support to all officers and technical staff in FIST Laboratory. I also want truthfully thanks to Central Laboratory staffs for their service with the instrumental facilities.

I would like to express the deepest gratitude to my family. Mom, Dad, and my only sister, for all provided support, encouragement and interest in my thesis work. Thanks for listening to my problems and providing advices when I need it. I would not be who am I today without you all.

I am also grateful to my partners and classmates, who supported me through ups and downs for years.

## ABSTRACT

This thesis purpose is to define the phase formation and electrical properties of Sodium Bismuth Titanate Doped by Barium Titanate using various ratios. The BNT is a candidate material for future dielectric and piezoelectric applications that cover large temperature ranges. BNT based materials are being studied to create an alternative of PZT that can meet the current industry standard. The present work encompasses the structural, microstructural, functional group, density and impedance analysis on BNT lead-free ceramics synthesized in the frequency range 1 kHz-30 MHz. Powder X-ray diffraction pattern derived from the resulting data at the room temperature subjected to Rietveld refinements and Williamson-Hall plot analysis confirmed the formation of phase pure compound. The FESEM micrograph images of the samples showed dense microstructure and uniform grain size. Fourier Transform Infrared Spectroscopy related to the change of dipole moment and the possible of transition of energy levels. Then, Archimedes Principles testing showed the porosity present in the pallets and last, Impedance Analysis plots showed the dielectric constant ( $\epsilon'$ ) and dielectric loss ( $\tan \delta$ ) decreased as the frequency increased.

## ABSTRAK

Tujuan kajian ini adalah untuk menentukan pembentukan fasa dan sifat elektrik Natrium Bismut Titanate Doped Barium Titanate dengan menggunakan pelbagai nisbah. BNT adalah bahan calon dielektrik dan piezoelektrik aplikasi masa depan yang meliputi julat suhu yang besar. Bahan-bahan berasaskan BNT sedang dikaji untuk alternatif selain PZT yang boleh memenuhi standard industri semasa. Kajian yang merangkumi struktur, mikrostruktur, kumpulan berfungsi, ketumpatan dan analisis impedans pada BNT seramik plumbum disintesis dalam julat frekuensi 1kHz-30MHz. Powder X-ray corak pembelauan yang diperolehi daripada data yang diperolehi pada suhu bilik dan tertakluk kepada Rietveld penghalusan Williamson-Hall analisis plot mengesahkan pembentukan fasa sebatian tulen. The FESEM imej mikrograf sampel menunjukkan mikrostruktur padat dan saiz butiran seragam. Fourier Transform Infrared Spektroskopi yang berkaitan dengan perubahan dipole masa dan kemungkinan tahap peralihan tenaga. Kemudian, ujian Prinsip Archimedes menunjukkan keliangan di dalam palet dan terakhir, Analisis Impedance plot menunjukkan dielektrik malar ( $\epsilon'$ ) dan kehilangan dielektrik ( $\tan \delta$ ) menurun selaras dengan frekuensi meningkat.

## TABLE OF CONTENTS

	<b>Page</b>
<b>SUPERVISORS' DECLARATION</b>	<b>iii</b>
<b>STUDENT'S DECLARATION</b>	<b>iv</b>
<b>DEDICATION</b>	<b>v</b>
<b>ACKNOWLEDGEMENTS</b>	<b>vi</b>
<b>ABSTRACT</b>	<b>vii</b>
<b>ABSTRAK</b>	<b>viii</b>
<b>TABLE OF CONTENTS</b>	<b>ix</b>
<b>LIST OF TABLES</b>	<b>xi</b>
<b>LIST OF FIGURES</b>	<b>xii</b>
<b>LIST OF SYMBOLS</b>	<b>xiii</b>
<b>LIST OF ABBREVIATIONS</b>	<b>xiv</b>
<b>CHAPTER 1            INTRODUCTION</b>	<b>1</b>
1.1    BACKGROUND RESEARCH	1
1.2    PROBLEM STATEMENT	3
1.3    OBJECTIVE OF RESEARCH	3
1.4    SCOPE OF STUDY	3
<b>CHAPTER 2            LITERATURE REVIEW</b>	<b>5</b>
2.1    INTRODUCTION TO CERAMIC	5
2.2    PIEZOELECTRICITY	5
2.3    FERROELECTRIC CERAMIC	6
2.4    SODIUM BISMUTH TITANATE	7
2.4.1    Previous study of BNT	8
2.5    BARIUM TITANATE	8
2.5.1    Perovskite Structure	8
2.6    BNT DOPING WITH BT	9
2.7    SOL-GEL METHOD	9
2.7.1    Technique of Sol-gel	10

<b>CHAPTER 3</b>	<b>METHODOLOGY</b>	11
3.1	SAMPLE PREPARATION	11
3.1.1	Sodium Bismuth Titanate	11
3.1.2	Barium Titanate	12
3.1.3	BT Doped into BNT Solution	12
3.2	SAMPLE CHARACTERIZATION	12
3.2.1	X-Ray Diffraction	12
3.2.2	Field Effect Electron Microscopy	14
3.2.3	FTIR Spectroscopy	14
3.2.4	Impedance Study	15
3.2.5	Density	15
3.3	FLOW CHART	16
<b>CHAPTER 4</b>	<b>RESULT AND DISCUSSION</b>	17
4.1	PHASE FORMATION AND STRUCTURE	17
4.1.1	Structural Study	17
4.1.2	FTIR Spectroscopy	22
4.1.3	Microstructural Study	24
4.1.5	Density	29
4.2	ELECTRICAL PROPERTIES	29
4.2.1	Impedance Study	29
4.3	CONCLUSION	31
<b>CHAPTER 5</b>	<b>SUMMARY AND RECOMMENDATION</b>	
5.1	SUMMARY	33
5.2	RRECOMMENDATION	34
<b>REFERENCES</b>		35
<b>APPENDIX</b>		37

## LIST OF TABLES

Table	Title	Page
Table 4.1	Average of crystallite sizes from different sample based on Williamson-Hall analysis	22
Table 4.2	Average of grain sizes from different composition BNT:BT	28
Table 4.3	Measurement of density and apparent porosity of BNT:BT with different ratios	29
Table 4.4	Values of dielectric constant and dielectric loss from frequency 1000Hz	31
Table 4.5	Result from different characterization testing	32

## LIST OF FIGURES

Figure	Title	Page
Figure 2.5	Perovskite structure of BT	9
Figure 2.7	Sol-Gel method process	10
Figure 3.2	Williamson-Hall plot	13
Figure 4.1.1	XRD patterns for various composition	18
Figure 4.1.1(a)	XRD pattern for BNT-BT with ratio 98:2	19
Figure 4.1.1(b)	XRD pattern for BNT-BT with ratio 96:4	19
Figure 4.1.1(c)	XRD pattern for BNT-BT with ratio 94:6	20
Figure 4.1.1(d)	XRD pattern for BNT-BT with ratio 92:8	20
Figure 4.1.1(e)	Williamson-Hall Plot for 98:2 BNT:BT	21
Figure 4.1.1(f)	Williamson-Hall Plot for 96:4 BNT:BT	21
Figure 4.1.1(g)	Williamson-Hall Plot for 94:6 BNT:BT	21
Figure 4.1.1(h)	Williamson-Hall Plot for 92:8 BNT:BT	22
Figure 4.1.2	FTIR spectrum of BNT without doping with BT	23
Figure 4.1.2(a)	FTIR spectrum of BNT with various composition doping with BT	24
Figure 4.1.3	BNT with different ratios under FESEM with 50.0kX magnification	25
Figure 4.1.3(a)	BNT-BT ratio 100:0 with different magnification	26
Figure 4.1.3(b)	BNT-BT ratio 98:2 with different magnification	26
Figure 4.1.3(c)	BNT-BT ratio 96:4 with different magnification	27
Figure 4.1.3(d)	BNT-BT ratio 94:6 with different magnification	27
Figure 4.1.3(e)	BNT-BT ratio 92:8 with different magnification	28
Figure 4.2.1(a)	Frequency dependence of dielectric constant and dielectric loss of BNT in room temperature	30

## LIST OF SYMBOLS

~	-	approximately
%	-	percent
$\lambda$	-	wavelength
$\mu$	-	micron ( $10^{-6}$ )
$2\theta$	-	Bragg angle
$^{\circ}\text{C}$	-	degree celcius
$\text{\AA}$	-	angstrom ( $10^{-10}$ )
g	-	grams
h	-	hour
$t$	-	time
$\epsilon'$	-	dielectric constant
Hz	-	frequency
$\tan \delta$	-	dielectric loss

## LIST OF ABBREVIATIONS

XRD	-	X-ray diffraction
FTIR	-	Fourier transform spectroscopy
FESEM	-	Field emission scanning electron microscope
BNT	-	Sodium Bismuth Titanate
BT	-	Barium Titanate
PZT	-	Lead Zirconate Titanate

## CHAPTER 1

### INTRODUCTION

#### 1.1 BACKGROUND RESEARCH

Today, lead zirconate titanate powder (PZT) are the utmost generally utilized for different modern operations because of their astounding piezoelectric properties. Ultimately, it is surely understood that PZT ceramics are environmentally burdened materials since it produces toxic PbO during sintered with high temperature. In this way, the examination focused on how to supplant PZT with another material that lead-free piezoelectric ceramics. They concentrated on this matter as the results of natural issues emerging from the lead poisonous quality. Among the free lead piezoelectric ceramics production,  $\text{Bi}_{0.5}\text{Na}_{0.5}\text{TiO}_3$  or BNT is expected to replace PZT due the developing worry with ecological contamination (Wu et al., 2011)

BNT is one of a perovskite structure that displays high Curie temperature ( $T_c = 320\text{ }^\circ\text{C}$ ) furthermore solid ferroelectric impact with a broadly comprehensive polarization ( $P_r = 38\text{ }\mu\text{C}/\text{cm}^2$ ) at room temperature. For some reason, a sol-gel technique used to get ready BNT-BT creation. Sol-gel is a strategy for delivering strong materials from little particles. The technique is utilized for the manufacture of metal oxides. It experiences the drawbacks of chemical inhomogeneity prominent to particle size for the component. Sol-gel technique has favorable circumstances over current solid-state method such as multi-component system can desirable with high homogeneity (Mercadell et al., 2008)

The sol-gel operation known as an arrangement of an oxide system through polycondensation reactions of an atomic forerunner in a liquid. A sol, steady scattering of colloidal particles in a stable. The components may be amorphous or crystalline. For utmost part, the sol particles collaborated by van der Waals strengths or hydrogen bonds. A gel may likewise be framed from connecting polymer chains. In gel frameworks utilized for materials combination, the associations are of a equivalent nature and the gel procedure is permanent. Amidst these processes the based citrate-nitrate sol-gel burning procedure is a method to deliver multicomponent oxide clay powders in a straightforward and financial way. Nowadays, this technique, has been utilized to create uniform and exceedingly receptive crystalline powders. The sol-gel process prompts accomplish a consistent cations appropriation by crosslinking a concentrated arrangement of carboxylate-metal buildings into a 3D gel.

The combustion synthesis, portrayed by huge temperatures, quick warming rates, and brief response times, responses between an oxidizer (metal nitrates) and a fuel (citric extract), manage started in a furnace at the temperature lower than 500 °C. The extract assumes two essential parts: it is the fuel for the burning response and it shapes durable buildings with metal particles keeping the precipitated hydroxylated mixes. In addition, citrate gel gives off an impression of being the minimum hazardous and, along these lines, generally more secure fuel (Badapanda et al., 2013)

The fundamental objective of this trial was to set up the better amalgamation parameters expected to create fine BNT-BT powders by citrate-nitrate sol-gel ignition method. In any case, there is no writing wrote about the arrangement and electrical properties of BNT samples, that have somewhat ferroelectric properties have slightly ferroelectric properties have been reported. A few reports on BNT-BT synthesis using sol-gel method are published. BaTiO<sub>3</sub> ceramics are prepared and doped into a solution for maintaining a strategic distance from the loss of Bi and Na amid the sintering process Bi<sub>0.5</sub>Na<sub>0.5</sub>TiO<sub>3</sub> by sol-gel strategy (Mercadelli et al., 2008)

## **1.2 PROBLEM STATEMENT**

Once, strong arrangement of lead PZT are the huge broadly utilized for piezoelectric applications because of magnificent piezoelectric properties. Despite, the investigation is recently on lead-free piezoelectric ceramics, as an outcome of ecological controversy emerging from the lead harmfulness (Reichmann, Feteira, & Li, 2015). BNT-based ceramics production demonstrates an incredible prospect for ecological security as well as for different application, particularly in the piezoelectric application. However, real disadvantage connected with BNT is that it has exceptionally poor sinterability which confines its applications. The present of intrinsic point defects as well as loss of volatile compounds when sintered at high temperature. Accordingly, to enhance the properties of BNT production, Barium Titanate ( $\text{BaTiO}_3/\text{BT}$ ) was acquainted for dopping with BNT. As this solid-solution formed, BNT-BT, as examined by demonstrated a decent pooling conduct and hence fascinating piezoelectric properties.

## **1.3 OBJECTIVES OF RESEARCH**

The objective of this research are:

1. To prepare Sodium Bismuth Titanate (BNT) doped by Barium Titanate ( $\text{BaTiO}_3$ ) ceramics by using a sol-gel method.
2. To determine the phase formation and structure of Sodium Bismuth Titanate doped by Barium Titanate.
3. To determine the electrical properties of Sodium Bismuth Titanate doped by Barium Titanate.

## **1.4 SCOPE OF STUDY**

Sodium Bismuth Titanate and Barium Titanate are used in this research. There is some modification composition of Sodium Bismuth Titanate which doped by different ratio of Barium Titanate using a sol-gel method.

Various composition with different ratio are prepared then this composition will be sintered and pelletized. Then, the samples are ready for testing their characteristics. A method such as Fourier Transform Spectroscopy (FTIR), the two molecules are regulated with the molecules' characteristics absorption of infrared radiation. Next, Field Emission Scanning Electron Microscopy (FESEM) is used for contributes topographical and elemental data. Then, X-ray Diffractometer (XRD), the phase compositions in a quantitative way are described. The XRD arrangements of the MPB compositions in the  $2\theta$  ranges. Furthermore, for characterizing and determine the electrical properties of the samples, Electrical Impedance Analysis is used. Finally, Archimedes principle also applied to determine their densities and any porosities.

## **CHAPTER 2**

### **LITERATURE REVIEW**

#### **2.1 INTRODUCTION OF CERAMIC**

There are two major categories of ceramics, traditional and advanced. Traditional applications include incorporate items like dinnerware or ovenware and development items like tile or windows. The majority of these applications have been being utilized for quite a while and thusly markets are grown-up with single digit improvement. Advanced applications exploit particular mechanical, electrical, synthetic properties of glass or clay materials and have entered the scene in the course of the most recent quite a few years. The business sectors for some of these applications can have twofold digit development. Ferroelectric(FE) and piezoelectric properties of BNT was examined and reported. NBT are firmly ferroelectric materials with generally high Curie temperatures of 653 and 593 K, separately additionally, pyroelectric properties of BNT was reported for a positive temperature coefficient of resistivity impact was seen insoluble bismuth titanates. This impact was completely researched by a few authors (Abdullah & Das-Gupta, 1990)

#### **2.2 PIEZOELECTRICITY**

The word piezoelectricity means electricity resulting from pressure. At the point when a dimensional change is forced on the dielectric, polarization occurs and a voltage or field is made which is termed as a direct effect. Then, the use of an electric field to a

dielectric, likewise bring about dimensional a change which is termed as reverse impact. Dielectric materials shows this reversible conduct are piezoelectric(Shi & Yang, 2009) PZT is known as the most universal used piezoelectric ceramics with strong arrangement between lead zirconate ( $\text{PbZrO}_3$ ) known as PZ and Lead Titanate ( $\text{PbTiO}_3$ ) known as PT. For their phenomenal piezoelectric properties, they are utilized at the morphotropic phase boundary. In any cases, lead and its compounds are generally toxic. The scientists wanting to confine the utilization of dangerous materials, such as lead as well as other heavy metals due to the toxic effects of lead and its compounds. However, there is no comparable substitute for PZT and its utilization still proceeded. This may be a temporary respite, yet the enactment absolutely inspired the specialists to create elective without lead piezoelectric materials keeping in mind the end goal to supplant toxic materials. Accordingly, scientists are currently investigating a few classes of materials which are possibly appealing distinct options for PZT for applications like BNT and BT ceramics.

### **2.3 FERROELECTRIC CERAMIC**

Ferroelectric ceramics were found in polycrystalline barium titanate. Since then, a consistent progression of recent materials and improvements that have prompted a critical mechanical's number and business utilizations. The ferroelectrics ceramics Sodium Bismuth Titanate(BNT) and Barium Titanate(BT), portrayed as the concept of the hysteresis loop, pointed as reason on lead-free materials are in no time in the most astounding purpose of excitement for ferroelectric and piezoelectric materials. Ferroelectric ceramics had piezoelectric reaction over the poling process exhibited in this part. Nowadays, the predominant opinion was that ceramics could not be piezoelectrically dynamic, in light of the fact that the arbitrarily arranged dipoles would, all in all, offset each other. One of the basic probes in the comprehension of ferroelectricity and piezoelectricity in ceramics was the disclosure of bizarrely high dielectric steady of BT(Hu et al., 2013)

BNT, are found indicates as solid ferroelectric properties with an essentially remaining polarization of  $38 \mu\text{C}/\text{cm}^2$ , and a Curie temperature of  $320 \text{ }^\circ\text{C}$ . Besides, it deprivations such as high conductivity and huge coercive field ( $\sim 73 \text{ kV}/\text{c}$ ). Then, the BNT ceramic needs a high sintering temperature ( $\sim 1000 \text{ }^\circ\text{C}$ ) to get thick specimens (Roy et al., 2013). It is felt that the vaporization of  $\text{Bi}^{+3}$  particles happened amid the sintering process at temperatures higher than  $1200 \text{ }^\circ\text{C}$ , achieving the poor poling meds in perspective of the high conductivity. There have been efforts to enhance the piezoelectric reaction of BNT by the substitution of one or a greater prominent measure of its particles.

#### **2.4 SODIUM BISMUTH TITANATE (BNT)**

Sodium bismuth titanate (NBT or BNT) as solid inorganic compound of sodium, bismuth, titanium and oxygen with the synthetic of  $\text{Bi}_{0.5}\text{Na}_{0.5}\text{TiO}_3$ , which adopts the Perovskite structure. BNT is considered to be magnificent without lead piezoelectric ceramics competitor with a perovskite structure of rhombohedral symmetry at room temperature. BNT has high anisotropic electro-mechanical coupling property with the steady  $K_p = 16.5\text{-}25.5 \%$  in plane course and  $K_t \geq 48 \%$  in thickness bearing, high recurrence consistent  $N_t \geq 2550 \text{ Hz}\cdot\text{m}$  and lower room temperature dielectric constant around 290-524 that simply take care of the ultrasonic application. Hence, BNT-based ceramics show incredible probability for ecological assurance as well as for different applications (Reichmann et al., 2015)

However, the major drawback associated with BNT is that it has exceptionally poor sinterability which limits its applications. The presence of intrinsic point defects, as well as the loss of volatile compounds, occurs when sintered at high temperature. So, to upgrade the properties of BNT ceramics, it is necessary it is important to decrease the sintering temperature or enhance the densification of ceramics. The low sintering temperature is required to keep up the stoichiometry or ostensible organization alongside the decrease of energy consumption.

### **2.4.1 Previous study of BNT**

On past study, BNT is prepared by solid state reaction route with conventional sintering for simple blend and ease. Different sintering strategies have been adjusted by means of non-customary sintering procedures, for example, spark plasma sintering, microwave sintering, multi-step sintering, and reactive sintering. Nonetheless, these sintering procedures have their own particular limitations. The conventional solid-state method is need high calcination temperature and repeated grinding. Thus, a basic strategy with low sintering temperature and moderately modest feedstock required for the arrangement the astounding BNT based lead-free piezoelectric ceramics.

## **2.5 BARIUM TITANATE (BT)**

BT as inorganic compound with the synthetic equation  $\text{BaTiO}_3$  is a white powder and transparent as larger crystals. Among BNT based solid states, the BNT-BT system has rhombohedral-tetragonal MPB in the range of 0.06-0.07 mol BT that uncovers moderately high piezoelectric and ferroelectric properties at the composition (Mercadelli et al., 2008)

Nonetheless, BNT cross section will affect the  $T_c$  moving to a lower temperature, which recommended that the materials were not suitable for high-temperature applications by doping BT with super high  $T_c$  at about 1000 °C, the  $T_c$  of BNT-BT ceramics will be expended correspondingly. Besides,  $\text{BaTiO}_3$  as one of the  $\text{ABO}_3$ -sort ferroelectrics has been generally used to adjust the BNT based materials. This work proposes that the MPB have existed in BNT-BT ceramics production at the BNT rich. As a rule, the multicomponent arrangement of piezoelectric materials will be effective to enhance the piezoelectric properties.

### **2.5.1 Perovskite Structure**

Perovskite structure is a material with the same kind of gem structure as calcium titanium oxide ( $\text{CaTiO}_3$ ) with the oxygen in the face focuses.

The perovskite structure received by numerous oxides that have the confection equation  $ABO_3$ . In the admired cubic unit cell of such a compound, sort "A" molecule sits at 3D square corner positions (0, 0, 0), sort "B" particle sits at body focus position (1/2, 1/2, 1/2) and oxygen ions sit at face focused positions (1/2, 1/2, 0). The subsequent electric dipole is in charge of the property of ferroelectricity and appeared by perovskites(Tang et al., 2004)

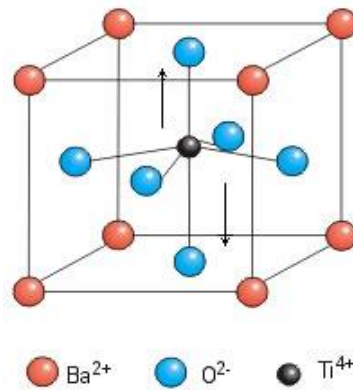


Figure 2.5 Perovskite Structure of  $BaTiO_3$

## 2.6 BNT DOPING WITH BT

NBT ceramics are extremely hard to post in view of their generally vast coercive field ( $E_c = 73$  kV/cm), prompting piezoelectric properties too low for usage. Amidst these strong arrangements,  $BaTiO_3$ -NBT (BNBT) framework has demonstrated a decent poling conduct and subsequently fascinating piezoelectric properties(Badapanda et al., 2013) Then, a morphotropic phase boundary (MPB) in this system have recorded a giant strain in the BNT-BT based system. The FE-AFE phase transformation is accompanied by a large volume and a large polarization change has reported dielectric properties of the  $(Bi_{0.5}Na_{0.5})TiO_3$ - $BaTiO_3$  single crystals and ceramics(Do et al., 2011)

## 2.7 SOL-GEL METHOD

In materials science, the sol-gel process is a method for producing solid materials from small molecules. The method is used for the fabrication of metal oxides, especially the oxides of silicon and titanium.

The process involves conversion of monomers into a colloidal solution (sol) that acts as the precursor for an integrated network (or gel) of either discrete particles or network polymers. Typical precursors are metal alkoxides.

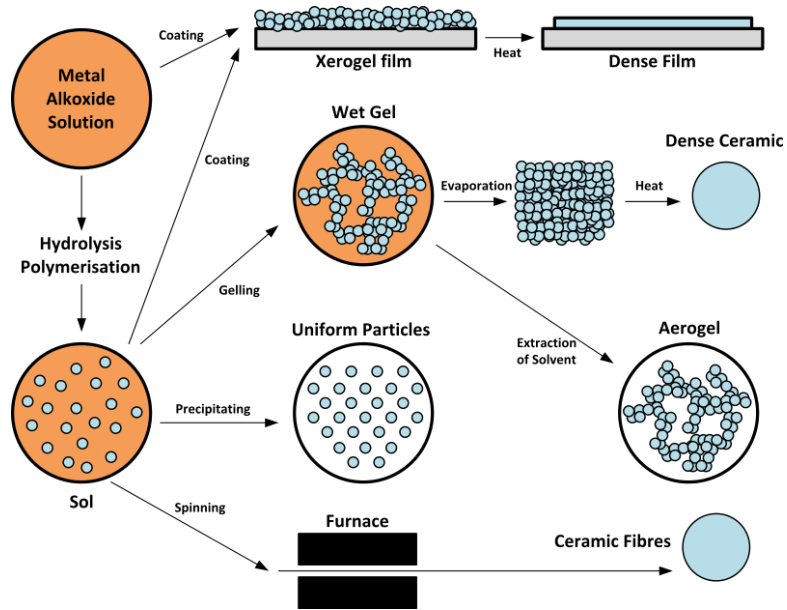


Figure 2.7 Sol-Gel method processes

### 2.7.1 Technique of Sol-Gel

In this chemical technique, the solution evolves towards the formation of a gel-like diphasic framework including both a liquid phase and solid phase whose morphologies range from discrete particles to continuous polymer networks. Evacuation of the liquid stage requires a drying process, which is typically accompanied by a significant amount of shrinkage and densification. The rate at which the solvent can be removed is ultimately determined by the conveyance of porosity in the gel. The definitive microstructure of the final component will clearly be strongly influenced by changes imposed upon the structural. The firing process to improve mechanical properties and structural stability via final sintering, densification and grain growth. The sol-gel approach is a modest and low-temperature strategy that allows for the fine control of the product's chemical composition. Indeed, small quantities of dopants, can be introduced in the sol and end up consistently dispersed in the finalise product.

## CHAPTER 3

### METHODOLOGY

#### 3.1 SAMPLE PREPARATION

Materials needed for this research are Sodium Acetate ( $\text{Na}(\text{CH}_3\text{COO})$ ), Titanium (IV) Butoxide ( $\text{Ti}(\text{OCH}_2\text{CH}_2\text{CH}_2\text{CH}_3)_4$ ), Bismuth (III) Acetate ( $(\text{CH}_3\text{CO}_2)_3\text{Bi}$ ), and Barium Acetate ( $(\text{Ba}(\text{C}_2\text{H}_3\text{O}_2)_2$ ). Acetic Acid, 2-methoxyethanol, ethanolamine, and acetylacetone also needed in appropriate amounts as solvents. Sample preparation divided into two parts for produced Sodium Bismuth Titanate (BNT) and Barium Titanate (BT).

##### 3.1.1 Sodium Bismuth Titanate

Firstly, Sodium Acetate diluted with 2-methoxyethanol by using magnetic stir for 30 minutes with 600 rpm. In the meantime, Bismuth (III) Acetate diluted with acetic acid and deionized water then stir for 30 minutes with 600 rpm. Then, combine the two solution and stir for about 15 minutes with 600 rpm. Next, Titanium (IV) Butoxide added, drop by drop and stir for about 15 minutes again with same rpm but added temperature of 70 °C. Finally, some acetylacetone was added and stir for 15 minutes with 600 rpm in thermal temperature. After that, it has been let to dry for 24 hours before being put for calcine three hours and turn to powder.

### 3.1.2 Barium Titanate

Next, for produce BaTiO<sub>3</sub>, mixed Barium Acetate with Acetic acid and water for 24 hour and stirred. Six drops of ethanolamine was added after 23 hours, then Titanium (IV) Butoxide after one hour. Then let it be gel after two days. After that the gel has been put for calcine three hours and it turn to powder.

### 3.1.3 BT are doped into BNT solution

After being sintered for three hours with maximum temperature 100 °C, combination of BNT-BT with different composition (100:0 , 98:2 , 96:4 , 94:6 , 92:8) were prepared. After sintering for three hours for 1000 °C, in the condition of powder, some were pelletize into 10 pellets with two samples of each composition and ready for various testing.

## 3.2 SAMPLE CHARACTERIZATION

### 3.2.1 X-ray Diffraction (XRD)

The purity of a sample can be determined by X-ray diffraction, as well as the composition of any impurities present. For this testing, the samples powder are taken for sintering for a few days then ready for XRD testing. The phase purity and the crystal structure were considered using X-ray powder diffractometer with Cu(K $\alpha$ ) ( $\lambda = 1.5402$  Å) radiation, over a wide range of Bragg angle ( $20^\circ \leq 2\theta \leq 60^\circ$ ) with a scanning speed of  $1^\circ \text{ min}^{-1}$  at room temperature. To determine the size and strain of the material, William-Hall Plot was used. It relies on the principle that the approximate formula for size broadening,  $\beta_L$ , and strain broadening,  $\beta_e$ , vary quite differently with respect to Bragg angle,  $\theta$ :

$$\beta_L = \frac{K\lambda}{D \cos\theta}$$

$$\beta_e = C\varepsilon \tan\theta$$

Using the former of these then can get:

$$\beta = \beta_e + \beta_L = C\varepsilon \tan\theta + \frac{K\lambda}{D \cos\theta}$$

If multiply this equation by  $\cos\theta$ :

$$\beta \cos\theta = C\varepsilon \sin\theta + \frac{K\lambda}{D}$$

and comparing this to the standard equation for a straight line ( $m = \text{slope}$ ;  $c = \text{intercept}$ )

$$y = mx + c$$

by plotting  $\beta \cos\theta$  versus  $\sin\theta$  we obtain the strain component from the slope ( $C\varepsilon$ ) and the size component from the intercept ( $K\lambda/D$ ). Such a plot is known as a Williamson-Hall plot and is illustrated schematically below:

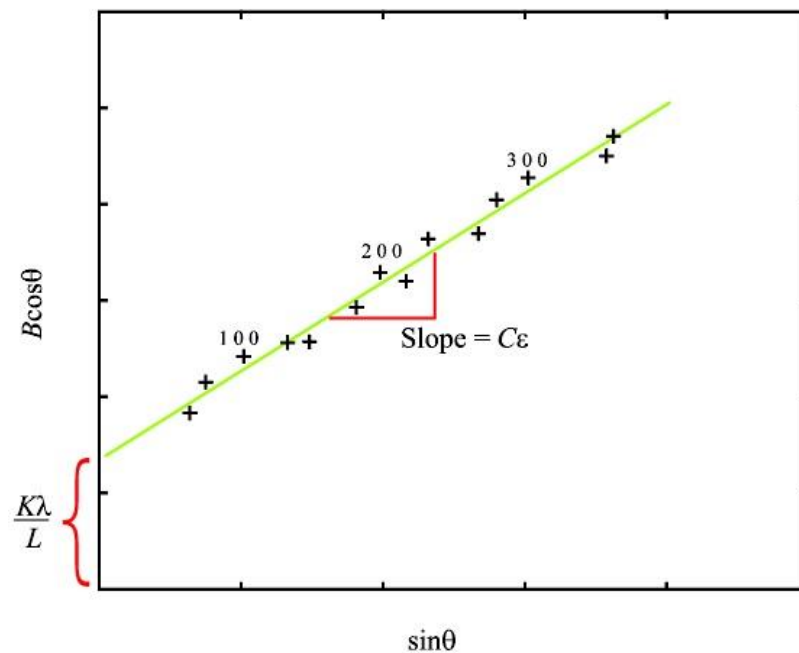


Figure 3.2 Williamson-Hall plot

### **3.2.2 Field Effect Scanning Electron Microscopy (FESEM)**

Field emission scanning electron microscopy (FESEM) provides topographical and elemental information with the unlimited depth of field. Compared with conventional scanning electron microscopy (SEM), FESEM produces clearer, less electrostatically distorted images. The principle of FESEM is based on the field emission cathode in the electron gun of scanning electron microscope provides however beam of electrons which when strikes the sample the secondary electrons, X-rays and backscattered electrons are ejected from the sample. These electrons are collected by the detector which gives the information about the sample by converting into signal that displays on screen.

### **3.2.3 FTIR Spectroscopy**

Utilization the structures of particles by using Fourier transform infrared spectroscopy with the atoms' trademark retention of infrared radiation. The frequency of the absorption peak is figured by the vibrational energy gap. The main goal of IR spectroscopy analysis is to determine the chemical functional groups in the sample. Different functional groups absorb characteristic frequencies of IR radiation. In this research of finding the functional group, spectroscopic tools by St. Thomas was used. Thus, by examining the infrared range, copious structure data of a particle is resolved. In this, a thin pellet was scanned for absorption spectra, which was made by using a pinch of powder sample and spectroscopic graded KBr as an infrared transparent material. The wave number range, used to record the FTIR spectrum of the sample at room temperature was  $400 \text{ cm}^{-1}$  to  $4000 \text{ cm}^{-1}$ .

### 3.2.4 Impedance Study

The ac impedance analysis has been found to be a powerful tool to separate out the grain boundary and grain-electrode effects, which usually are the sites of trap for oxygen vacancies and other defects. It is also useful in establishing space charge polarization and its relaxation mechanism, by aptly assigning different values of resistance and capacitance to the grain and grain boundary effects.

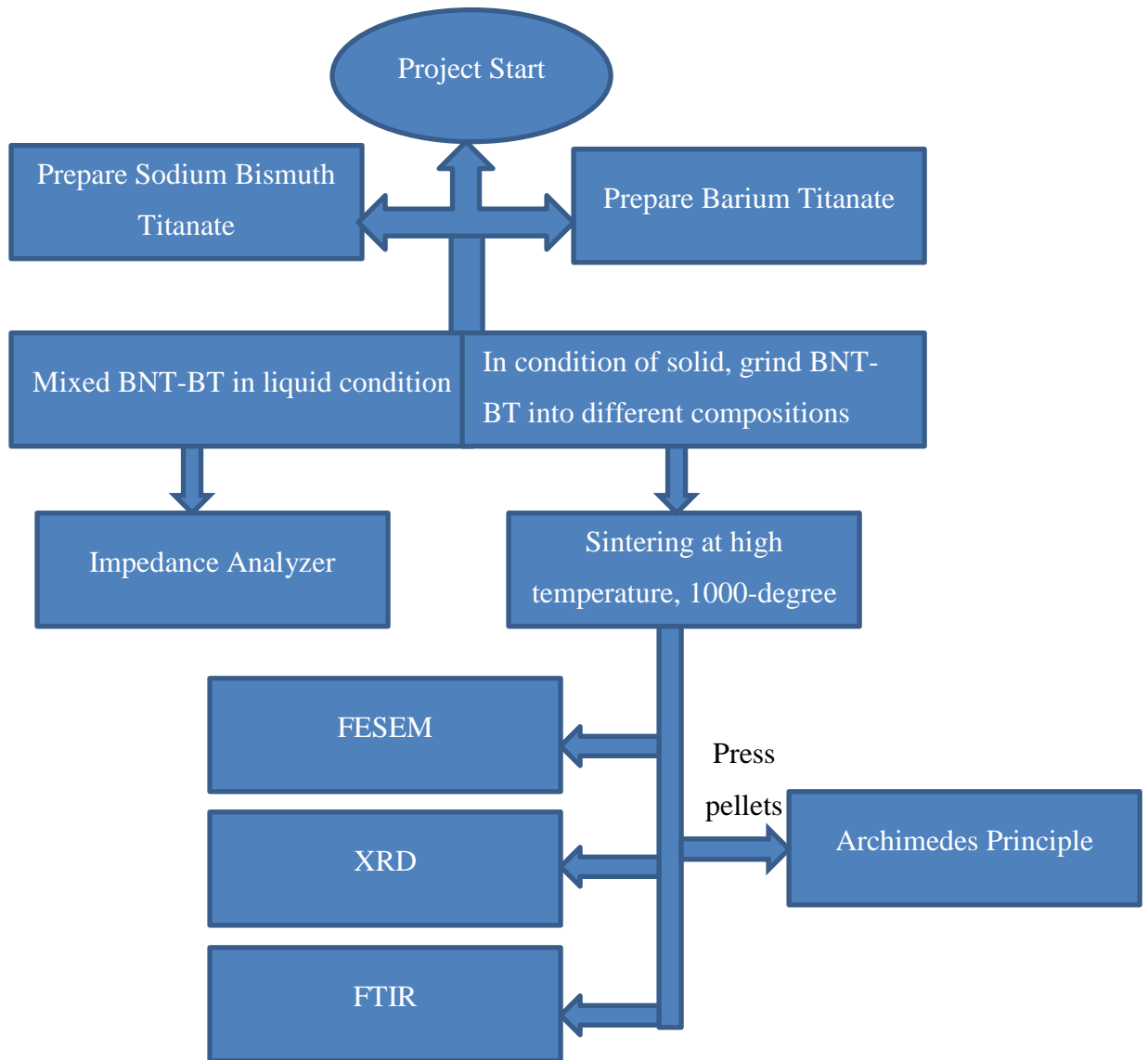
### 3.2.5 Density

The density of the sintered sample can be measured by following Archimedes principle. At first the dry weights of the sintered pallets were measured in weight balance machine. Then the pallets were soaked in glass beaker containing deionized water. Then the pallets in deionized water was taken and then were dried using filter paper to remove soaked weight and the measurement taken by weight balance machine after dry. So the bulk density can be given by

$$\text{Bulk Density} = (\text{Dry weight}) / (\text{soaked weight} - \text{suspended weight})$$

$$\text{Apparent porosity} = (\text{soaked weight} - \text{Dry weight}) / (\text{soaked weight} - \text{suspended weight})$$

### 3.3 FLOW CHART



## CHAPTER 4

### RESULT AND DISCUSSION

#### 4.1 PHASE FORMATION AND STRUCTURE

The properties of BNT- BT ceramics derived from sol-gel are smaller than those of samples produced by conventional solid state reaction method, due to the grain size and oxygen vacancies that generates dipolar effect. The reduced grain size has influenced the dielectric and piezoelectric properties.

The densities and grain dimensions of Spark Plasma Sintered ceramics increase with the increasing doped by BT. Permittivity values also increases with the increase doped by BT. The dispersion of the permittivity and losses are characteristics to relaxor behavior of the ceramics.

##### 4.1.1 Structural Study

*Figure 4.1.1* shows the XRD pattern with various compositions. A standard computer was utilized with the program for XRD-profile analysis using Rietveld refinements. Compare to the original pure 100:0 BNT:BT, the presence of rhombohedral as well as tetragonal phase of different ratios of BNT-BT, respectively, is observed by the splitting of peaks between  $30.316^\circ$ - $32.887^\circ$  into (100) and (110) in the XRD patterns, as shown in *Figure 4.1.1(a)*. The highest peak seemed to be slightly shifted to the right as the ratio increase.

All the composition exhibit a pure perovskite structure and no second phase is observed which implies that BT ceramic has diffused into BNT lattices to form solid solution. The strain and component sizes or crystalline sizes were calculated using Williamson-Hall Plot and formula. From *Figure 4.1.1(b)* the pure BNT-BT presence as rhombohedral and tetragonal phase at the peak (012), (101), (104), (006), (024), (116) and (018). The calculated strain is 3.3337 and the crystalline size is 4.49 nm. From *Figure 4.1.1(c)* the pure BNT-BT presence as rhombohedral and tetragonal phase at the peak (100), (110), (111), (200), (210) and (211). The calculated strain is 2.3057 and the crystalline size is 3.55 nm. From *Figure 4.1.1(d)* the pure BNT-BT presence as rhombohedral and tetragonal phase at the peak (100), (110), (111), (200), (210) and (211). The calculated strain is 1.0192 and the crystalline size is 2.83 nm. From *Figure 4.1.1(e)* the pure BNT-BT presence as rhombohedral and tetragonal phase at the peak (100), (110), (111), (200), (210) and (211). The calculated strain is 1.7292 and the crystalline size is 1.93 nm. This showed the crystalline size becomes smaller as the ratio increased.

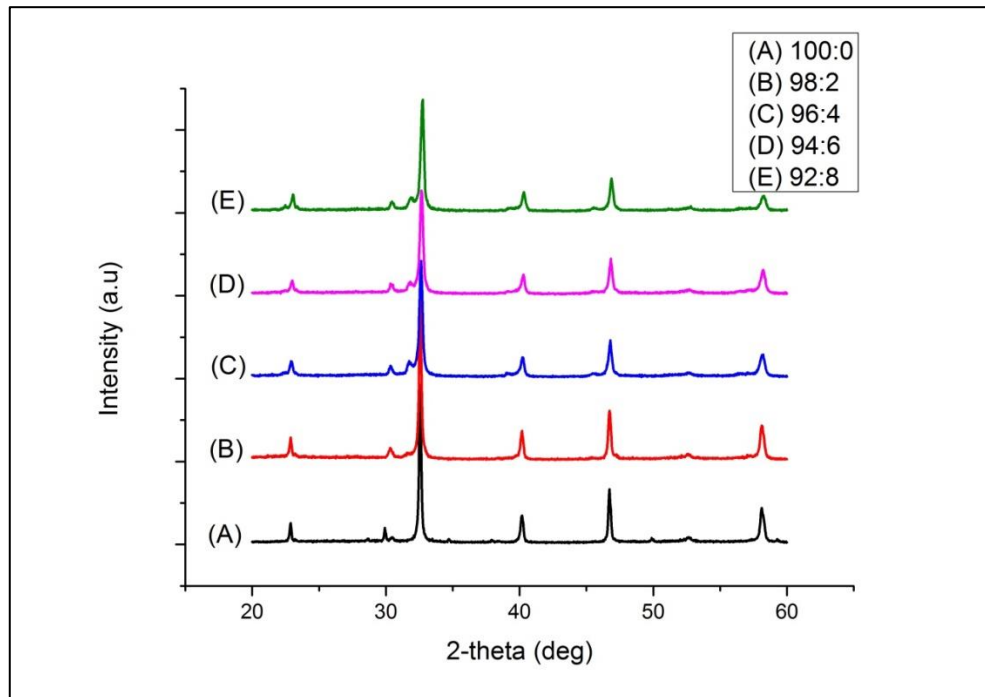


*Figure 4.1.1* XRD patterns for various compositions

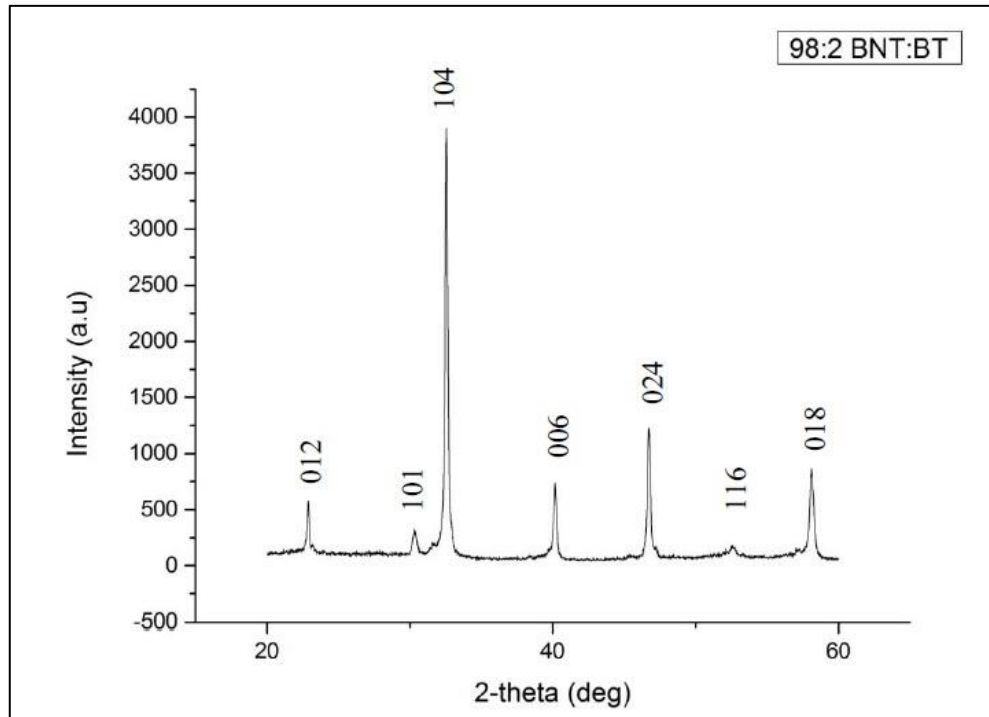


Figure 4.1.1(a) XRD pattern for BNT-BT with ratio 98:2

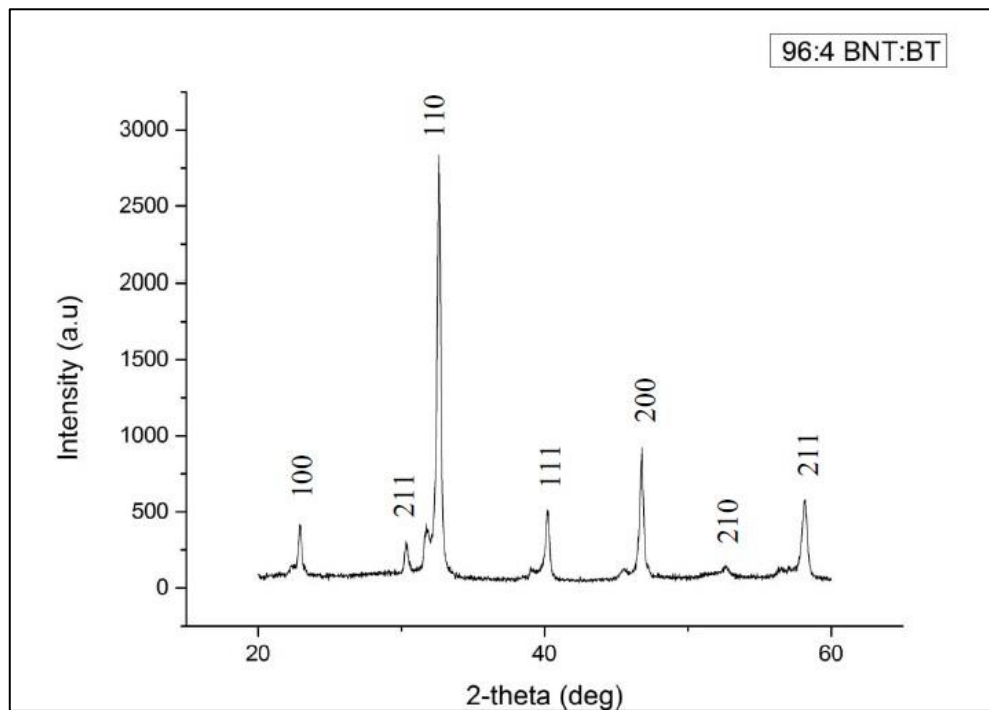


Figure 4.1.1(b) XRD pattern for BNT-BT with ratio 96:4

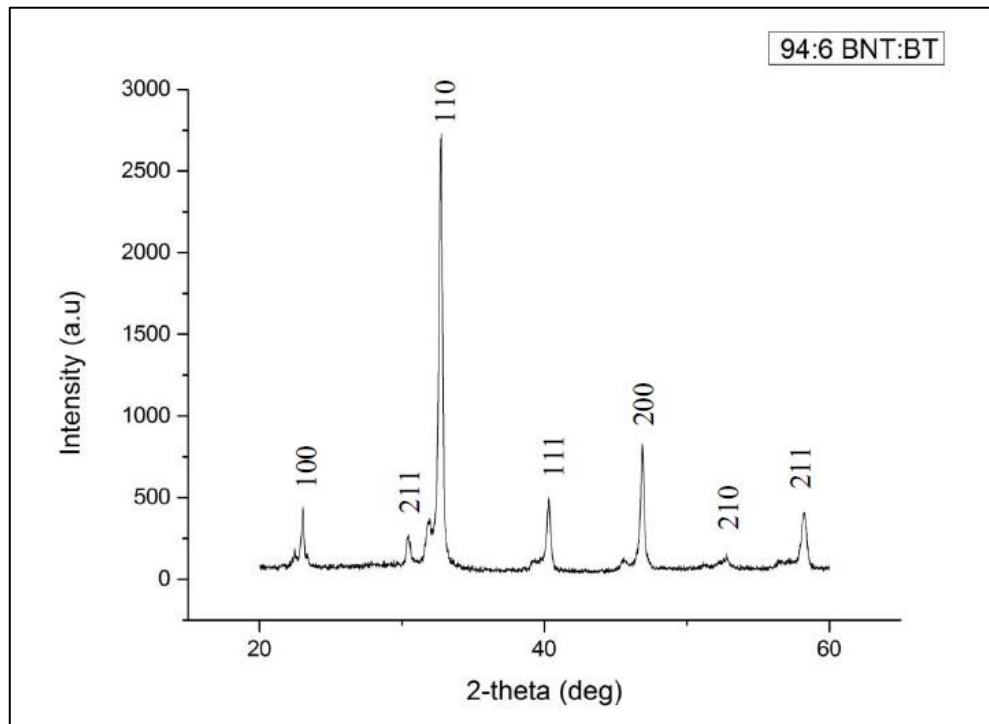


Figure 4.1.1(c) XRD pattern for BNT-BT with ratio 94:6

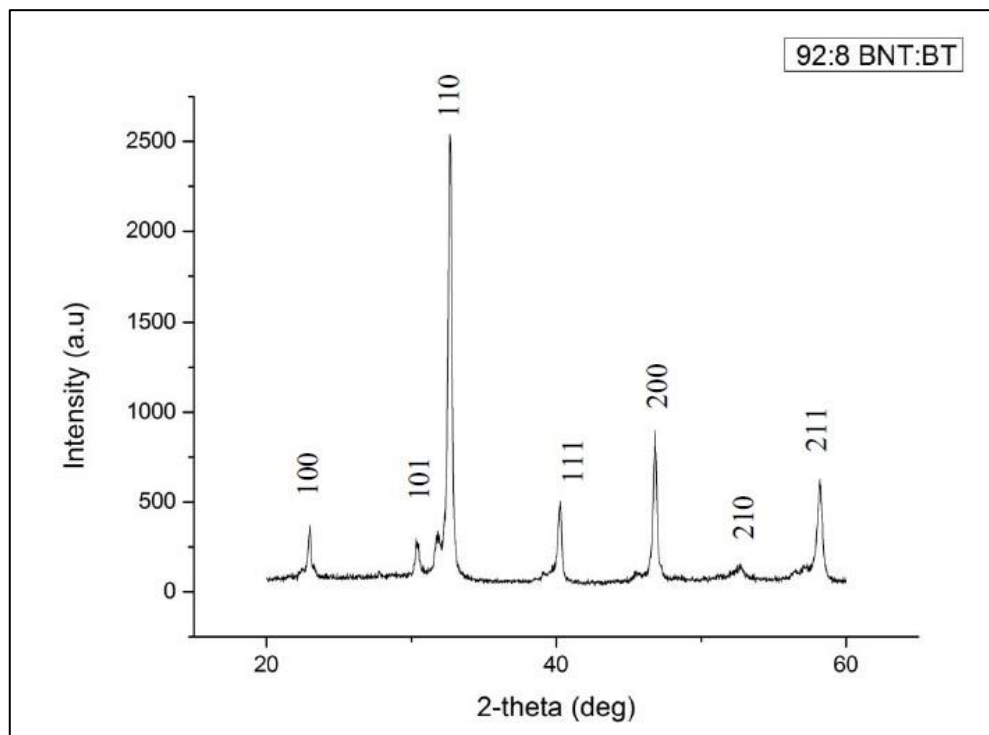


Figure 4.1.1(d) XRD pattern for BNT-BT with ratio 92:8

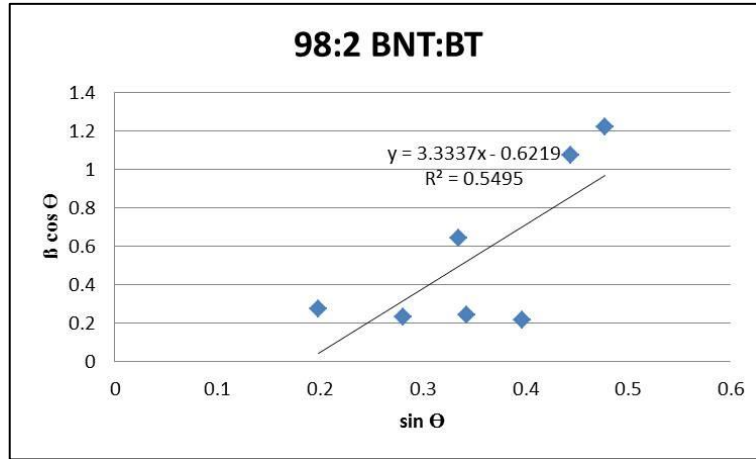


Figure 4.1.1(e) Williamson-Hall Plot for 98:2 BNT:BT

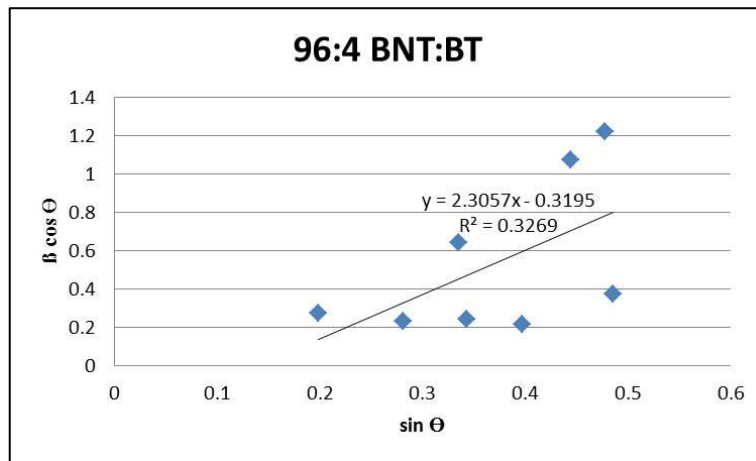


Figure 4.1.1(f) Williamson-Hall Plot for 96:4 BNT:BT

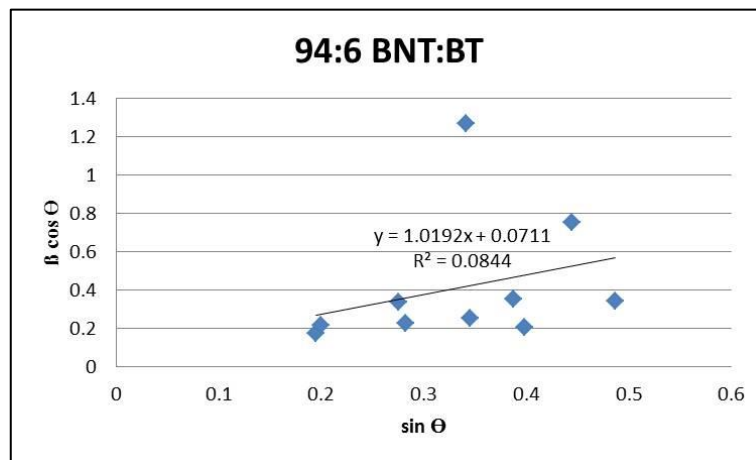


Figure 4.1.1(g) Williamson-Hall Plot for 94:6 BNT:BT

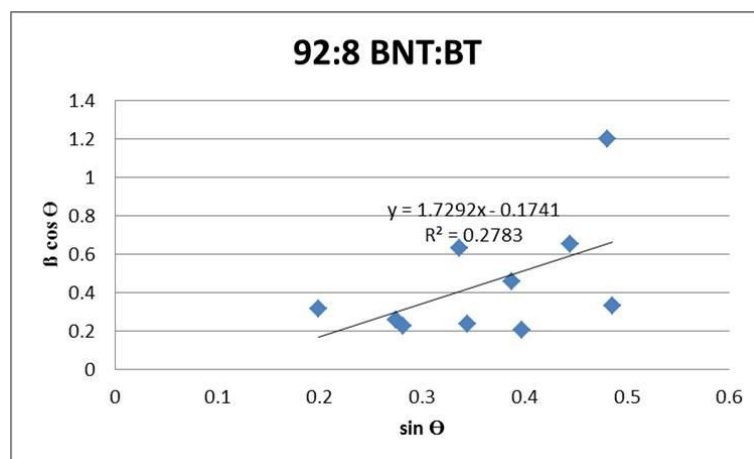


Figure 4.1.1(h) Williamson-Hall Plot for 92:8 BNT:BT

Table 4.1

Average crystallite size of different samples based on Williamson–Hall analysis

Sample	Crystallite size , D (nm)
98:2 BNT:BT	4.49
96:4 BNT:BT	2.31
94:6 BNT:BT	2.83
92:8 BNT:BT	1.93

#### 4.1.2 FTIR Spectroscopy

IR Spectrum used to identify Functional Groups that are present within a molecule. This is important because knowing the functional groups present brings closer to identifying an unknown substance and molecule. Based on the IR spectrum of pure 100 % BNT powder is shown in Figure 4.1.2. Three ranges were selected, the first range presenting C-H asymmetric deformation vibration at 1400 up to 1450  $\text{cm}^{-1}$ . At the second range 1700  $\text{cm}^{-1}$ ,  $\text{CH}_2$  wagging overtone presented as allene functional group. Then at the third range 3300~3340  $\text{cm}^{-1}$ , the C-H stretching vibration presented. As the BNT were doped by BT with composition of 98:2, 96:4, 94:6 and 92:8, the functional groups became complicated as showed in Figure 4.2(b).

Based on spectroscopic tools by St. Thomas, the the functional group of C-H deformation was observed present in three ratios 98:2 , 96:4 and 94:6 BNT:BT at their first selected wavelength ranges 575~975  $\text{cm}^{-1}$ . Then, for the second range of two ratios, 98:2 and 94:6, at 2100~2260  $\text{cm}^{-1}$  they showed the C-C stretching vibration. As for the third ranges, between 3580~3670  $\text{cm}^{-1}$  three ratios showed the same functional, known as O-H stretching vibration in 98:2 , 96:4 and 92:8 BNT:BT.

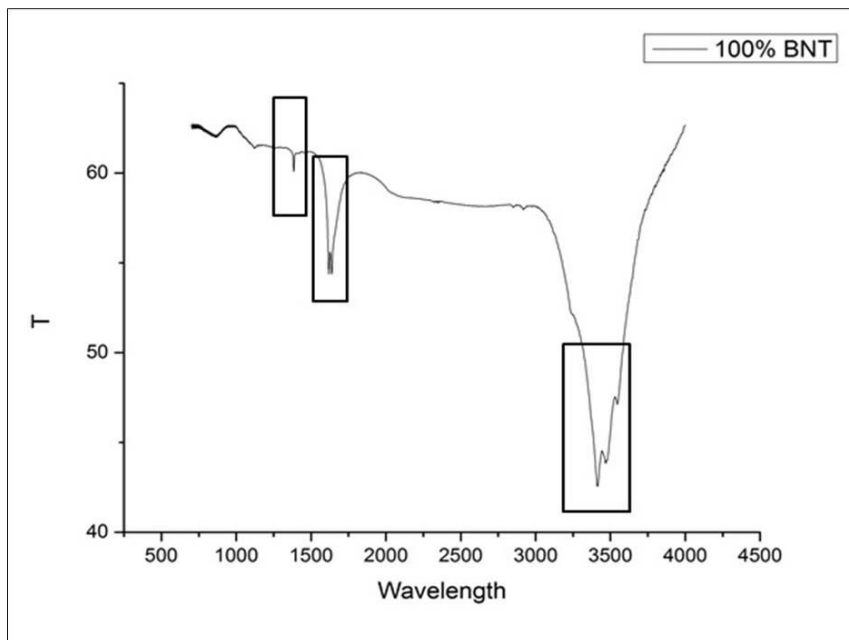


*Figure 4.1.2* FTIR spectrum of BNT without doping with BT

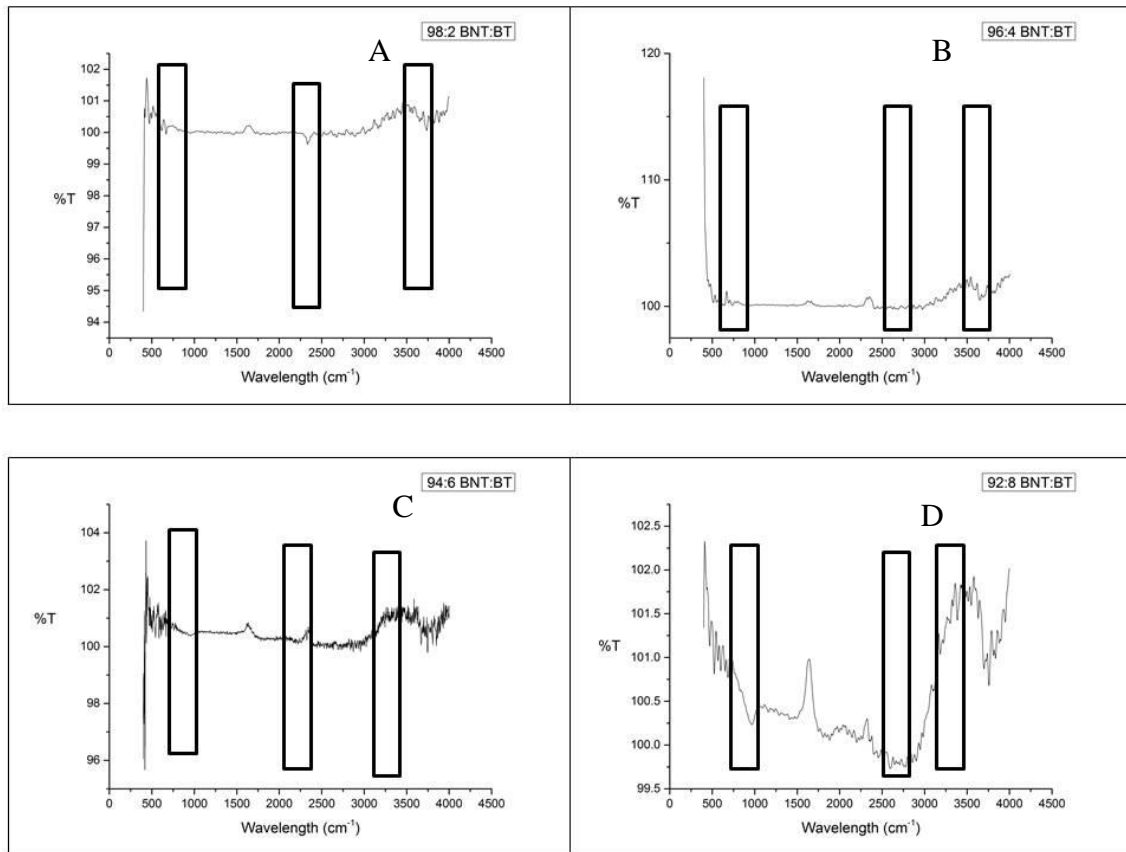
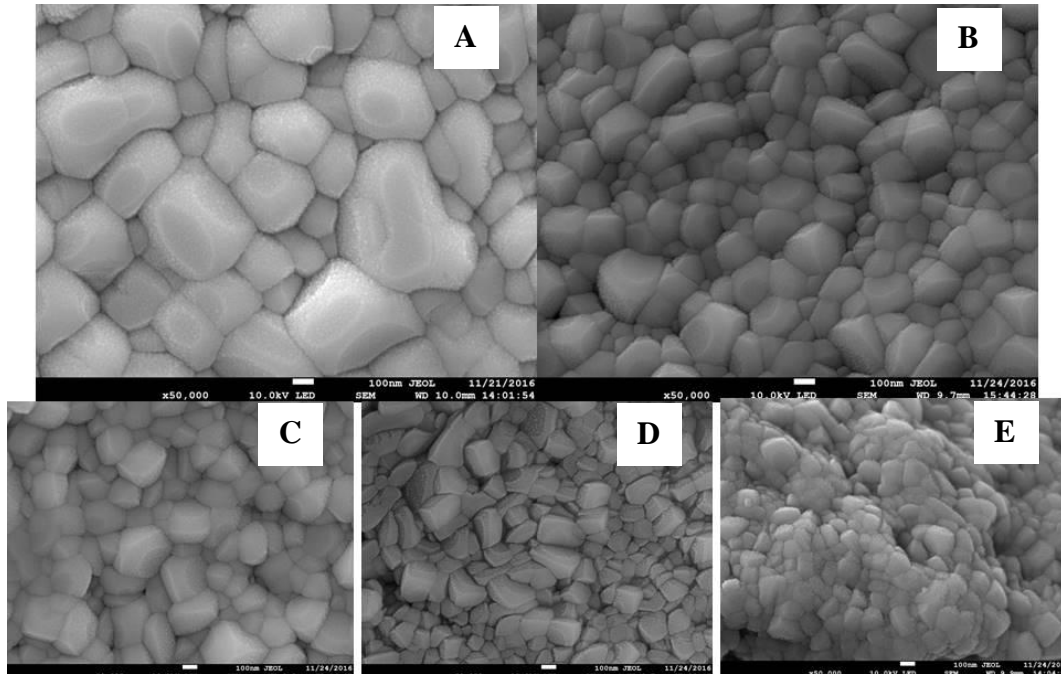


Figure 4.1.2(a) FTIR Spectrum of BNT with various composition doping with BT A) 98:2 B) 96:4 C) 94:6 D) 92:8

### 4.1.3 Microstructural Study

FESEM micrograph shows the polycrystalline nature of sample having spherical type of grain of different sizes and distributed non-uniformly throughout the sample surface. The images reveal the influence of the BaTiO<sub>3</sub> in BNT affect the grain size as showed in *Figure 4.1.3*. The grain sizes were measured by ImageJ program and shown in Table 4.2. The grain sizes decrease as the ratio increase. It showed BT affected the structure inside the BNT and increase the porosity then controlled the grain size too. This proved along the apparent porosity calculated in Table 4.3. Raw material resulted from sol-gel synthesis, sintered at 1000 °C, shows a relative uniform distribution with and the images under FESEM also tested in different magnification as showed in *Figure 4.1.3(b), 4.1.3(c), 4.1.3(d), 4.1.3(e), and 4.1.3(f)*.

On the contrary, the addition of BT results in the inhibition of grain growth, so the BNT-BT appears to be more uniform in both size and shape. It can also be seen that the grain size reduces with increase in BT content which is may be due to the  $Ba^{2+}$  abounds in crystal boundary prevents the ion from migrating and restrains the growing of grains.



*Figure 4.1.3* BNT with different ratios A)100 %BNT B)98 %BNT C)96 %BNT D)94 %BNT E)92 %BNT under FESEM with 50.0k X magnification

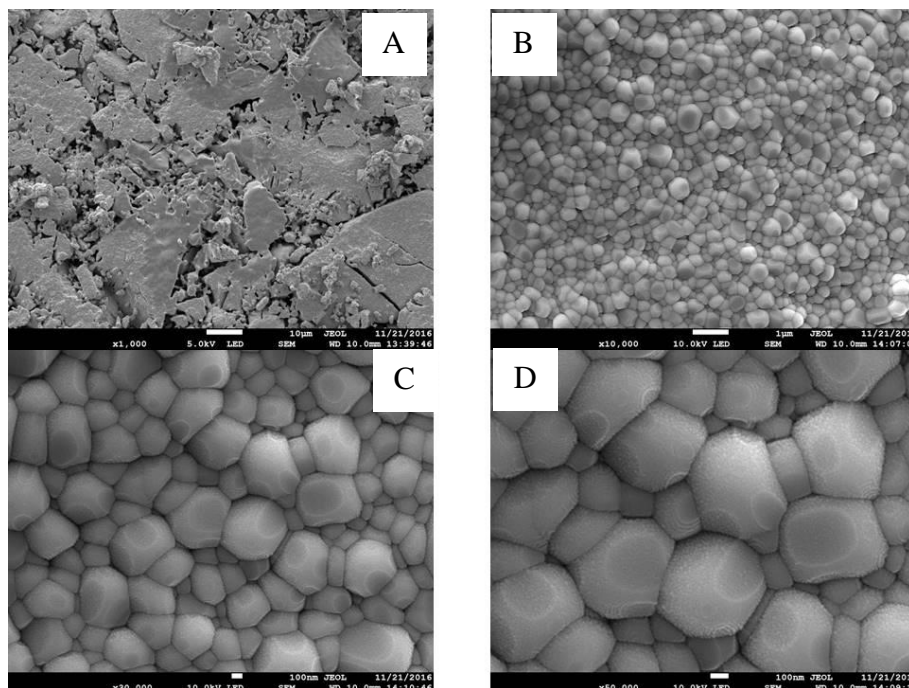


Figure 4.1.3(a) BNT-BT ratio 100:0 with different magnification A) 1.0k X B)10.0k X C)30.0k X D)50.0k X

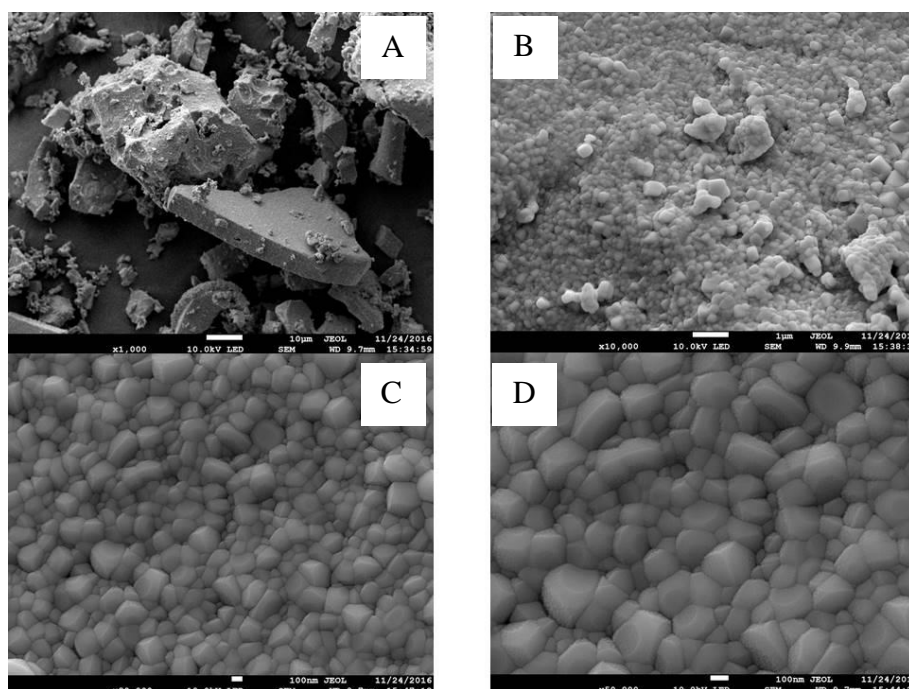


Figure 4.1.3(b) BNT-BT ratio 98:2 with different magnification A) 1.0k X B)10.0k X C)30.0k X D)50.0k X

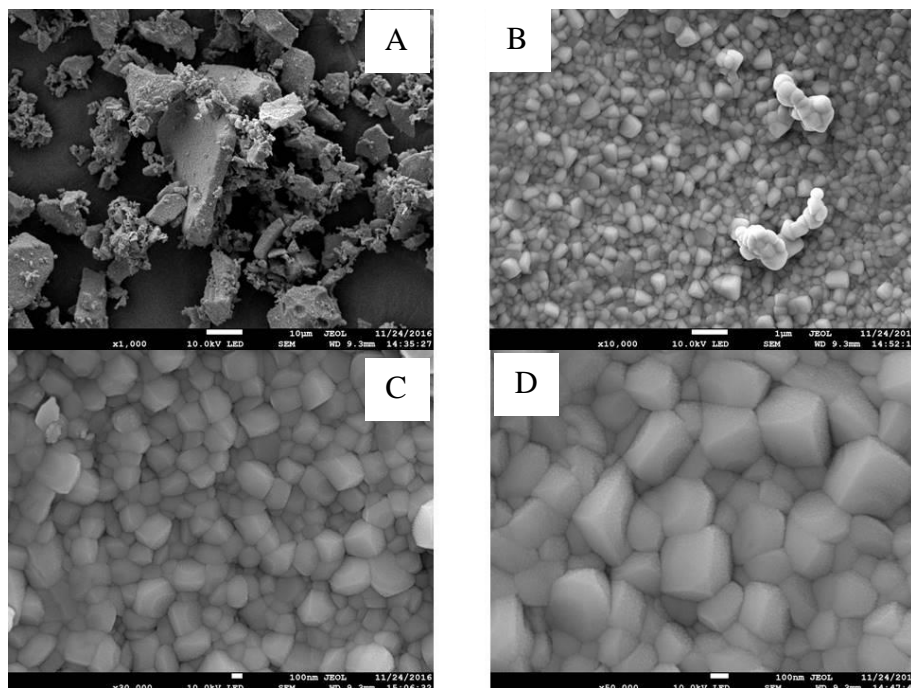


Figure 4.1.3(c) BNT-BT ratio 96:4 with different magnification A) 1.0k X B)10.0k X C)30.0k X D)50.0k X

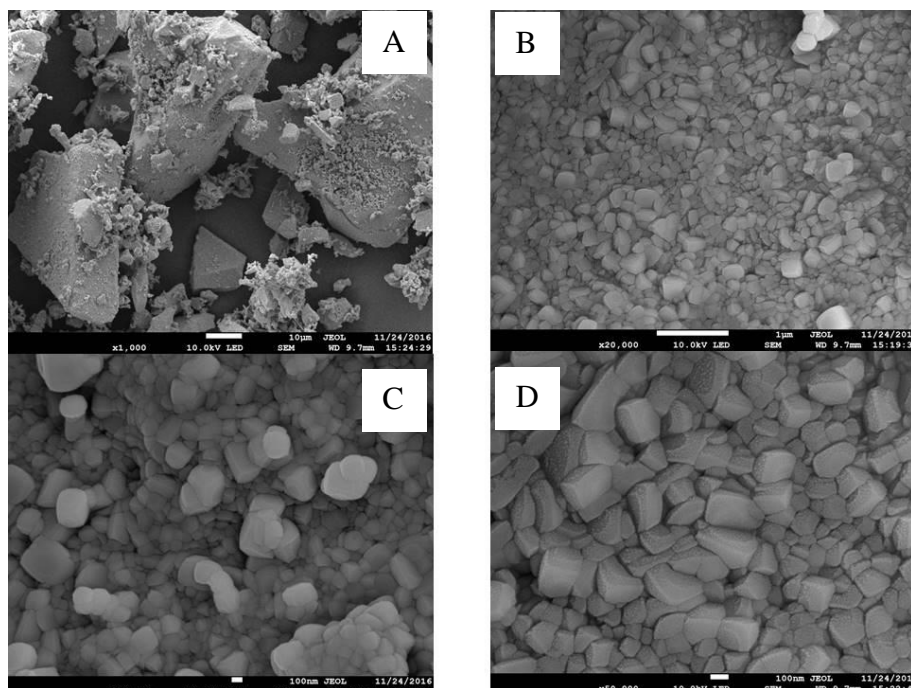


Figure 4.1.3(d) BNT-BT ratio 94:6 with different magnification A) 1.0k X B)10.0k X C)30.0k X D)50.0k X

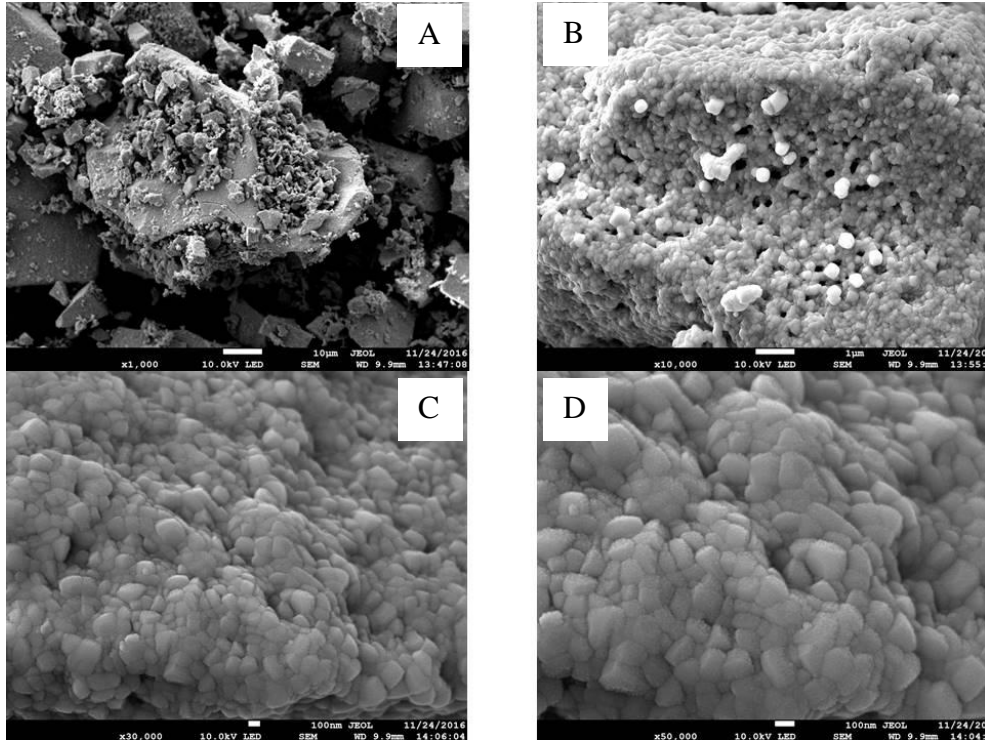


Figure 4.1.3(e) BNT-BT ratio 92:8 with different magnification A) 1.0k X B)10.0k X C)30.0k X D)50.0k X

Table 4.2

*Average of grain sizes from different composition BNT-BT*

Sample	Ratio (BNT:BT)	Area ( $\mu\text{m}^2$ )	Average of Grain Size ( $\mu\text{m}$ )
A)100% BNT	100:0	225.5	$166.1 \pm 8.3$
B)98% BNT	98:2	201.5	$141.8 \pm 9.3$
C)96% BNT	96:4	147.2	$132.3 \pm 13.6$
D)94% BNT	94:6	133.2	$110.5 \pm 13.5$
E)92% BNT	92:8	103.4	$110.5 \pm 11.7$

#### 4.1.4 Density

The density and apparent porosity of various composition on BNT-BT was shown in Table 4.3. The density increased as the ratios increased.

Table 4.3

*Measurement of density and apparent porosity of BNT-BT with different ratios*

Sample	Dry weight (g)	Soaked weight (g)	Suspended weight (g)	Bulk Density (g/cm <sup>3</sup> )	Apparent porosity
100 % BNT	0.9457	1.0513	0.9495	9.2852	1.0368
98 % BNT 2 % BT	0.9573	1.0511	0.9656	11.1965	1.0965
96 % BNT 4 % BT	0.9586	1.0557	0.9734	11.6406	1.1791
94 % BNT 6 % BT	0.9552	1.0522	0.9671	11.2244	1.1398
92 % BNT 8 % BT	0.9378	1.0288	0.9559	12.8642	1.2483

## 4.2 ELECTRICAL PROPERTIES

### 4.2.1 Impedance Study

Frequency dependence of dielectric constant and dielectric loss of BNT-BT ceramics solution measured at room temperature from 1000 Hz to 30 MHz by using the E4990A impedance analyzer as showed in Appendix. The results showed in Table 4.4(a) where the machine detect dielectric constant ( $\epsilon'$ ) and dielectric loss ( $\tan \delta$ ) for various composition BNT-BT. The graph automatically plotted by the computer showed the red line as dielectric constant and blue one was the imaginary parts. Dielectric loss quantifies a dielectric material's inherent dissipation of electromagnetic energy. It can be parameterized in terms of either the loss angle  $\delta$  or the corresponding loss tangent

$\tan\delta$ . The electric loss tangent can be similarly defined upon introduction of an effective dielectric conductivity as in *Figure 4.1.4(a)*. At frequency of 1000 Hz, the highest dielectric constant detected in composition of 94 % BNT and 6 % BT. It proves that the BT-doped in BNT improve their electrical properties and 94 % BNT composition seemed to be the most suitable ratio to improve the properties.

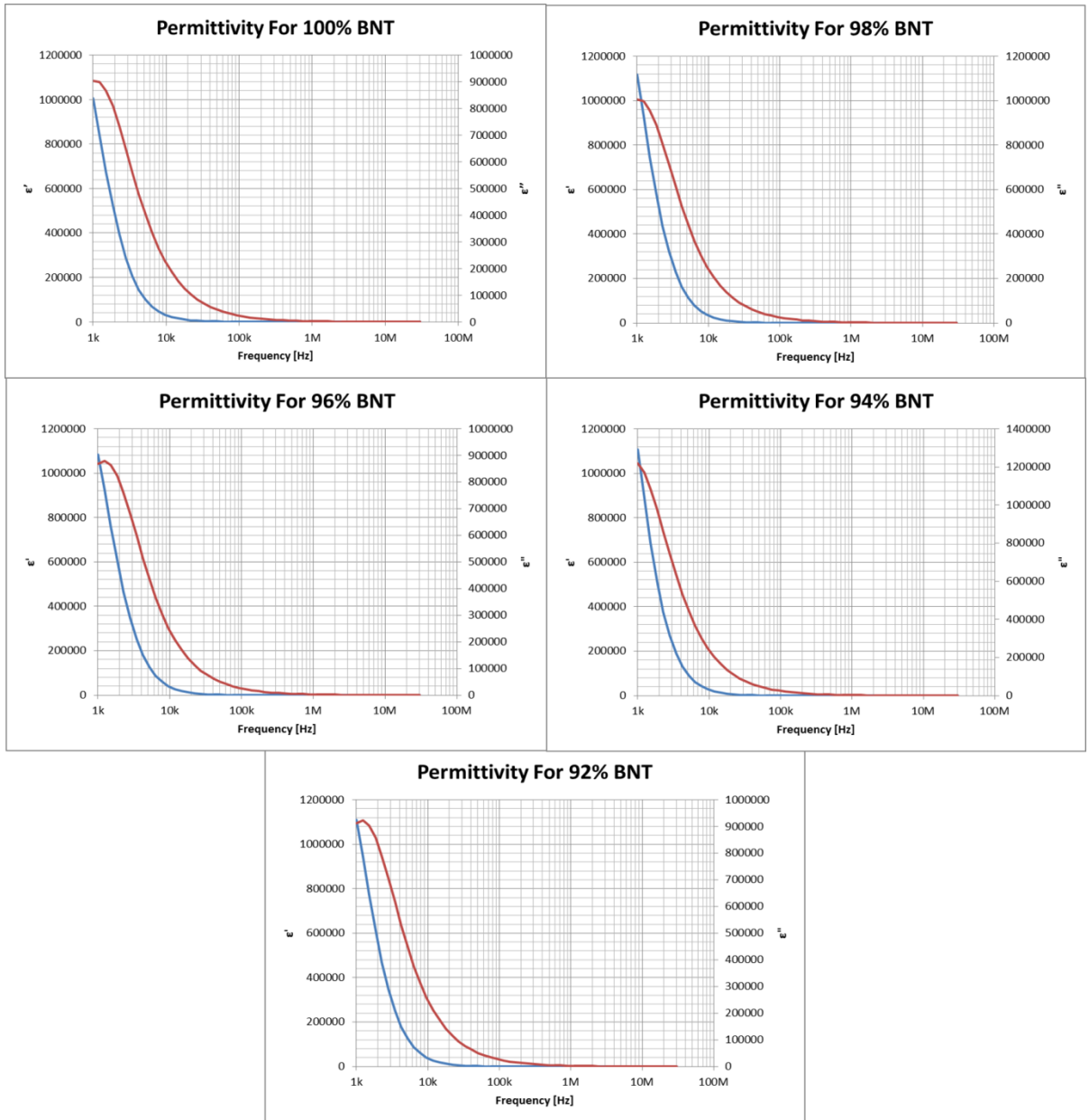


*Figure 4.2.1(a)* Frequency dependence of dielectric constant and dielectric loss of BNT in room temperature

Table 4.4

*Values of dielectric constant and dielectric loss from frequency 1000 Hz*

Samples	Dielectric constant ( $\epsilon'$ )	Dielectric loss ( $\tan \delta$ )
100 % BNT	1005709.7	0.899158315
98 % BNT	1084328.4	0.928121334
96 % BNT	1108534.9	0.823484055
94 % BNT	1116839.3	0.777951383
92 % BNT	1110604.4	1.098895528

### 4.3 CONCLUSION

BNT-BT ceramics were successfully prepared by sol-gel synthesis technique. The phase formation of BNT-BT were characterized by structural, microstructural, functional group and density testing. The result were different for every ratios. Dielectric constant decreases their values with the frequency increase for all ratios of BNT-BT. The dispersion of the permittivity and losses are characteristic to the relaxor behavior of the ceramics. Based on overall observations, BNT-BT with ratio of 94:6 seemed the best composition ceramic as the result obtained proved it. Table 4.4 showed overall results for every testing used in this research. As for the composition of BT increase, it enhance the BNT properties and the most suitable composition is 94:6 because it provide the smaller crystalline size and grain size but higher density and dielectric constant.

Table 4.5

*Result from different characterization testing*

Samples	Crystalline size (nm)	Grain size ( $\mu\text{m}$ )	Density ( $\text{g}/\text{cm}^3$ )	Dielectric constant ( $\epsilon'$ )
98 % BNT	4.49	$141.8 \pm 9.3$	11.1965	1084328.4
96 % BNT	2.31	$132.3 \pm 13.6$	11.6406	1108534.9
94 % BNT	2.83	$110.5 \pm 13.5$	11.2244	1116839.3
92 % BNT	1.93	$110.5 \pm 11.7$	12.8642	1110604.4

## CHAPTER 5

### SUMMARY AND RECOMMENDATION

#### 5.1 SUMMARY

The research meet it main objective to prepare Sodium Bismuth Titanate doped by Barium Titanate ceramic by using sol-gel technique, characterize and investigate the effect in different ratios on the ceramic. This chapter briefly outlines the summary of research and its limitation for improvement of future work.

- 1) By sol-gel technique, drying, and firing processes, BNT-BT successfully synthesized.
- 2) XRD pattern shows that a pure phase is obtained for BNT-BT by matching the peaks with ICDD data base roughly.
- 3) FESEM images show the microstructure of the material with small grain size as ratio increase and none uniformly spherical and round shapes distributed throughout the sample. The grain size were calculated automatically using imageJ.
- 4) Impedance studies for all the material in liquid solutions, showed the dielectric constant and dielectric loss variation decreased with frequency increased in room temperature.
- 5) By using Archimedes principle, the density can be calculated along with apparent porosity.

## 5.2 RECOMMENDATIONS

Each technique/steps of the process that dealt with preparation sol-gel, calcination and sintering must be done in appropriate manners. All the precautions must be correctly observed and followed to get the expected results. The recommendations for the future studies in this research topic are as follow:

- 1) Use different temperature on every ratio to find the most suitable sintering temperature to produce BNT-BT
- 2) In future study, do another testing to find the piezoelectric constant from the data results
- 3) Using more machine required to determine the electrical properties.

## REFERENCE

Abdullah, M. J., & Das-Gupta, D. K. (1990). Electrical Properties of Ceramic/Polymer Composites. *IEEE Transactions on Electrical Insulation*, 25(3), 605–610. <http://doi.org/10.1109/14.55739>

Badapanda, T., Venkatesan, S., Panigrahi, S., & Kumar, P. (2013). Structure and dielectric properties of bismuth sodium titanate ceramic prepared by auto-combustion technique. *Processing and Application of Ceramics*, 7(3), 135–141. <http://doi.org/10.2298/PAC1303135B>

Cernea, M., Andronescu, E., Radu, R., Fochi, F., & Galassi, C. (2010). Sol-gel synthesis and characterization of BaTiO<sub>3</sub>-doped (Bi<sub>0.5</sub>Na<sub>0.5</sub>)TiO<sub>3</sub> piezoelectric ceramics. *Journal of Alloys and Compounds*, 490(1), 690-69

Chicago Do, N. B., Lee, H. B., Yoon, C. H., Kang, J. K., Lee, J. S., & Kim, I. W. (2011). Effect of Ta-Substitution on the Ferroelectric and Piezoelectric Properties of Bi<sub>0.5</sub>(Na<sub>0.82</sub>K<sub>0.18</sub>)<sub>0.5</sub>TiO<sub>3</sub> Ceramics. *Transactions on Electrical and Electronic Materials*, 12(2), 64–67 <http://doi.org/10.4313/TEEM.2011.12.2.64>

Dai, Y. J., Pan, J. S., & Zhang, X. W. (2007). Composition Range of Morphotropic Phase Boundary and Electrical Properties of NBT-BT System. In *Key Engineering Materials* (Vol. 336, pp. 206-209). Trans Tech Publications.

Hu, D., Kong, X., Mori, K., Tanaka, Y., Shinagawa, K., & Feng, Q. (2013). Ferroelectric mesocrystals of bismuth sodium titanate: Formation mechanism, nanostructure, and application to piezoelectric materials. *Inorganic Chemistry*, 52(18), 10542–10551. <http://doi.org/10.1021/ic4015256>

Mercadelli, E., Galassi, C., Costa, A. L., Albonetti, S., & Sanson, A. (2008). Sol-gel combustion synthesis of BNBT powders. *Journal of Sol-Gel Science and Technology*, 46(1), 39–45. <http://doi.org/10.1007/s10971-008-1693-4>

Reichmann, K., Feteira, A., & Li, M. (2015). Bismuth Sodium Titanate based materials for piezoelectric actuators. *Materials*, 8(12), 8467–8495. <http://doi.org/10.3390/ma8125469>

Roy, A. K., Prasad, K., & Prasad, A. (2013). Piezoelectric, impedance, electric modulus and AC conductivity studies on  $(\text{Bi}_{0.5}\text{Na}_{0.5})_{0.95}\text{Ba}_{0.05}\text{TiO}_3$  ceramic. *Processing and Application of Ceramics*, 7(2), 81–91. <http://doi.org/10.2298/PAC1302081R>

Shi, J., & Yang, W. (2009). Piezoelectric and dielectric properties of CeO<sub>2</sub>-doped  $(\text{Bi}_{0.5}\text{Na}_{0.5})_{0.94}\text{Ba}_{0.06}\text{TiO}_3$  lead-free ceramics. *Journal of Alloys and Compounds*, 472(1-2), 267–270. <http://doi.org/10.1016/j.jallcom.2008.04.038>

Tang, X., Wang, J., Wang, X., & Chan, H. L. (2004). Preparation and Electrical Properties of Highly (111)-Oriented  $(\text{Na}_{0.5}\text{Bi}_{0.5})\text{TiO}_3$  Thin Films by a Sol–Gel Process. *Chemistry of Materials*, 16(25), 5293–5296. <http://doi.org/10.1021/cm0352221>

Wu, L., Xiao, D., Zhou, F., Teng, Y., & Li, Y. (2011). Microstructure, ferroelectric, and piezoelectric properties of  $(1-x-y)\text{Bi}_{0.5}\text{Na}_{0.5}\text{TiO}_3-x\text{BaTiO}_3-y\text{Bi}_{0.5}\text{Ag}_{0.5}\text{TiO}_3$  lead-free ceramics. *Journal of Alloys and Compounds*, 509(2), 466–470. <http://doi.org/10.1016/j.jallcom.2010.09.062>

## APPENDIX



Image 1 Part of raw material used to synthesize BNT and BT



Image 2 Colour changes upon times because the varying composition



Image 3 Impedance Analyzer